Reactivity of the Binuclear Hydride $[Fe_2(CO)_4(\mu\text{-}H)(\mu\text{-}CO)(\mu\text{-}PPh_2)(\mu\text{-}Ph_2PCH_2PPh_2)]$ to generate Phosphido and Hydroxide Moieties at the Diiron Centre†

Graeme Hogarth* and Mark H. Lavender
Chemistry Department, University College London, 20 Gordon Street, London WC1H 0AJ, UK

Thermolysis of $[Fe_2(CO)_4(\mu\text{-}H)(\mu\text{-}CO)(\mu\text{-}PPh_2)(\mu\text{-}dppm)]$ **1** (dppm = $Ph_2PCH_2PPh_2$) results in benzene loss *via* phosphorus–carbon bond cleavage yielding $[Fe_2(CO)_5(\mu\text{-}PPh_2)(\mu\text{-}PhPCH_2PPh_2)]$ **2**. In a number of other reactions of **1**, carbon monoxide and the hydride are replaced by three-electron donor ligands. Chromatography on alumina afforded the bridging hydroxide complex $[Fe_2(CO)_4(\mu\text{-}OH)(\mu\text{-}PPh_2)(\mu\text{-}dppm)]$ **3**, while thermolysis in the presence of secondary phosphines gave the bis(phosphido) complexes $[Fe_2(CO)_4(\mu\text{-}PPh_2)(\mu\text{-}PR_2)(\mu\text{-}dppm)]$ (R = Ph **4** or C_6H_{11} **5**). Complexes **2**–**4** have been characterised crystallographically. All show a diiron centre bridged by two *cis* three-electron donor ligands. Both **4** and **5** are fluxional on the NMR time-scale, the observed changes being ascribed to a 'rocking' of the phosphido-bridges and a 'twisting' of the diphosphine respectively.

We have recently described the synthesis of the binuclear hydride complex $[Fe_2(CO)_4(\mu\text{-}H)(\mu\text{-}CO)(\mu\text{-}PPh_2)(\mu\text{-}dppm)]$ **1** (dppm = $Ph_2PCH_2PPh_2$) *via* the oxidative addition of the phosphorus–hydrogen bond of diphenylphosphine to $[Fe_2(CO)_6(\mu\text{-}CO)(\mu\text{-}dppm)]$. It shows high reactivity towards a variety of unsaturated organics including primary alkynes, allene and ethyl diazoacetate.[1] These reactions are characterised by loss of carbon monoxide and insertion of the unsaturated organic into the hydride functionality yielding complexes of the general type $[Fe_2(CO)_4(\mu\text{-}X)(\mu\text{-}PPh_2)(\mu\text{-}dppm)]$, where X is the new three-electron donor ligand formed *via* the insertion reaction. Thus, for example, insertion of primary alkynes resulted in the regioselective formation of σ,η-vinyl complexes, that is where X = $CR{=}CH_2$ (R = Me or Ph). The driving force in these reactions thus appears to be the formation of the stable puckered $Fe_2(\mu\text{-}X)(\mu\text{-}PPh_2)$ core. Herein we describe further reactivity studies of **1**, in which the products are again characterised as containing the $Fe_2(\mu\text{-}X)(\mu\text{-}PPh_2)$ core. These complexes are formed however, not as a result of insertion into the hydride functionality, but rather *via* its loss.

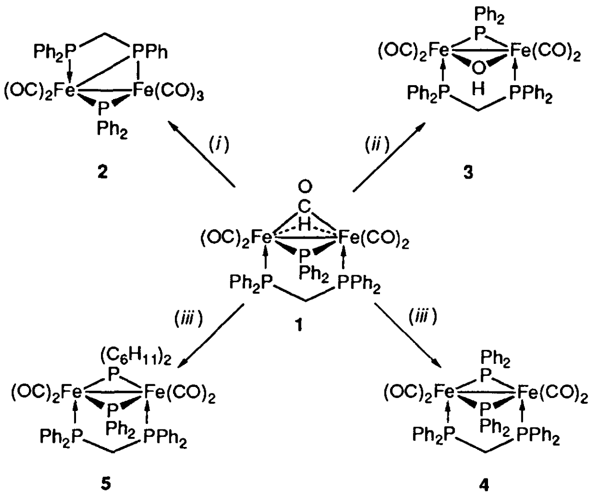

Scheme 1 (*i*) Toluene, 110 °C; (*ii*) chromatography on Al_2O_3; (*iii*) PR_2H, toluene, 110 °C

Results and Discussion

Synthesis and Characterisation.—While the diiron hydride complex $[Fe_2(CO)_4(\mu\text{-}H)(\mu\text{-}CO)(\mu\text{-}PPh_2)(\mu\text{-}dppm)]$ **1** is indefinitely stable at room temperature in deoxygenated solvents, thermolysis in toluene results in benzene loss and rapid formation of $[Fe_2(CO)_5(\mu\text{-}PPh_2)(\mu\text{-}PhPCH_2PPh_2)]$ **2** in 75% yield (Scheme 1). It is readily characterised on the basis of spectroscopic and analytical data, the latter indicating benzene loss. In the ^{31}P NMR spectrum (in $CDCl_3$) resonances at δ 171.1 (dd, *J* 153, 50), 103.7 (dd, *J* 153, 104) and 37.4 (dd, *J* 104, 50 Hz) are assigned to the two phosphido-bridge atoms and the diphosphine respectively. Examples of the cleavage of a phenyl ring from the dppm ligand are rare. Poilblanc and co-workers[2] have observed a facile phosphorus–aryl bond cleavage at a heterobimetallic ruthenium–rhodium centre. Here, however, the aryl ring is not lost as benzene, but rather is retained in the product, namely $[(dppm)(Ph)Ru(\mu\text{-}H)(\mu\text{-}Ph_2PCH_2PPh)Rh(cod)]$ (cod = cycloocta-1,5-diene). Transformation of dppm at triruthenium centres also leads to phosphorus–aryl bond cleavage and benzene loss, the resulting ligand capping three metal centres.[3,4] In previous work we have noted that facile phosphorus–methylene, as opposed to phosphorus–aryl, bond cleavage of dppm occurs at a diiron centre.[5] Thus, $[Fe_2(CO)_6(\mu\text{-}CO)(\mu\text{-}dppm)]$ transforms quantitatively into $[Fe_2(CO)_6(\mu\text{-}CH_2PPh_2)(\mu\text{-}PPh_2)]$ upon thermolysis in toluene. Competing phosphorus–aryl bond cleavage was however noted for the substituted diphosphine complex $[Fe_2(CO)_6(\mu\text{-}CO)\{\mu\text{-}Ph_2PCH(Me)PPh_2\}]$, thermolysis resulting in the isolation of $[Fe_2(CO)_6\{\mu\text{-}PhPCH(Me)PPh(C_6H_4\text{-}o)\}]$. This pronounced difference in reactivity upon methyl substitution was attributed to steric effects, the extra steric pressure at the carbon backbone pushing the phenyl substituents closer to the metal centre, thus facilitating phosphorus–aryl bond cleavage. It is possible that a similar steric effect may account for the reactivity observed here. Certainly there must be strong electronic effects leading to the preference for a *cis* orientation of phosphorus-containing ligands in **1**, since this will result in unfavourable steric interactions between phenyl rings.

Hydride loss from complex **1** does not necessarily require

---

† *Supplementary data available:* see Instructions for Authors, *J. Chem. Soc., Dalton Trans.*, 1993, Issue 1, pp. xxiii–xxviii.

Table 1 Selected bond lengths (Å) and angles (°) for $[Fe_2(CO)_5(\mu\text{-}PPh_2)(\mu\text{-}PhPCH_2PPh_2)]$ **2**

Fe(1)–Fe(2)	2.699(2)	Fe(2)–Fe(1)–P(1)	95.8(1)
Fe(1)–P(1)	2.224(3)	Fe(1)–Fe(2)–P(2)	52.7(1)
Fe(1)–P(2)	2.226(3)	Fe(2)–Fe(1)–P(2)	52.7(1)
Fe(2)–P(2)	2.227(3)	Fe(1)–Fe(2)–P(3)	51.4(1)
Fe(1)–P(3)	2.195(3)	Fe(2)–Fe(1)–P(3)	54.6(1)
Fe(2)–P(3)	2.287(3)	P(1)–Fe(1)–P(3)	149.9(3)
Fe(1)–C(4)	1.769(12)	P(2)–Fe(1)–P(3)	82.8(1)
Fe(1)–C(5)	1.744(11)	P(2)–Fe(2)–P(3)	80.8(1)
Fe(2)–C(1)	1.800(13)	P(1)–Fe(1)–P(2)	73.5(1)
Fe(2)–C(2)	1.781(11)	Fe(1)–P(2)–Fe(2)	74.6(1)
Fe(2)–C(3)	1.780(12)	Fe(1)–P(3)–Fe(2)	74.0(1)
P(1)–C(6)	1.844(10)	P(1)–C(6)–P(2)	91.9(5)
P(2)–C(6)	1.858(10)	Fe(1)–Fe(2)–C(1)	143.3(4)
P(1) ··· P(2)	2.661(4)	Fe(1)–Fe(2)–C(2)	102.1(4)
		Fe(1)–Fe(2)–C(3)	109.9(4)
		Fe(2)–Fe(1)–C(4)	110.2(4)
		Fe(2)–Fe(1)–C(5)	148.9(4)

Table 3 Selected bond lengths (Å) and angles (°) for $[Fe_2(CO)_4(\mu\text{-}PPh_2)_2(\mu\text{-}dppm)]$ **4**

Fe(1)–Fe(2)	2.713(2)	Fe(1)–Fe(2)–P(1)	52.7(1)
Fe(1)–P(1)	2.232(2)	Fe(2)–Fe(1)–P(1)	52.2(1)
Fe(2)–P(1)	2.218(2)	Fe(1)–P(1)–Fe(2)	75.1(1)
Fe(1)–P(2)	2.242(2)	Fe(1)–Fe(2)–P(2)	52.7(1)
Fe(2)–P(2)	2.250(2)	Fe(2)–Fe(1)–P(2)	53.0(1)
Fe(1)–P(3)	2.271(2)	Fe(1)–P(2)–Fe(2)	74.3(1)
Fe(2)–P(4)	2.223(2)	P(1)–Fe(1)–P(2)	79.8(1)
Fe(1)–C(1)	1.775(7)	P(1)–Fe(2)–P(2)	80.0(1)
Fe(1)–C(2)	1.761(6)	P(1)–Fe(1)–P(3)	146.2(1)
Fe(2)–C(3)	1.762(7)	P(1)–Fe(2)–P(4)	136.2(1)
Fe(2)–C(4)	1.748(7)	P(2)–Fe(1)–P(3)	92.9(1)
P(3)–C(5)	1.830(6)	P(2)–Fe(2)–P(4)	96.6(1)
P(4)–C(5)	1.832(6)	Fe(2)–Fe(1)–C(1)	111.9(2)
		Fe(2)–Fe(1)–C(2)	145.5(2)
		Fe(1)–Fe(2)–C(3)	122.8(2)
		Fe(1)–Fe(2)–C(4)	142.4(2)
		P(3)–C(5)–P(4)	112.2(3)

Table 2 Selected bond lengths (Å) and angles (°) for $[Fe_2(CO)_4(\mu\text{-}OH)(\mu\text{-}PPh_2)(\mu\text{-}dppm)]$ **3**

Fe(1)–Fe(2)	2.546(1)	Fe(1)–Fe(2)–P(1)	97.5(1)
Fe(1)–P(2)	2.250(2)	Fe(2)–Fe(1)–P(2)	97.2(1)
Fe(2)–P(1)	2.240(2)	Fe(1)–Fe(2)–P(3)	55.3(1)
Fe(1)–P(3)	2.223(2)	Fe(2)–Fe(1)–P(3)	54.5(1)
Fe(2)–P(3)	2.202(2)	P(1)–Fe(2)–P(3)	152.7(1)
Fe(1)–O(5)	2.224(4)	P(2)–Fe(1)–P(3)	151.7(1)
Fe(2)–O(5)	2.288(3)	P(1)–Fe(2)–O(5)	87.3(1)
Fe(1)–C(1)	1.762(8)	P(2)–Fe(1)–O(5)	85.9(1)
Fe(1)–C(2)	1.770(6)	P(3)–Fe(1)–O(5)	79.4(1)
Fe(2)–C(3)	1.761(7)	P(3)–Fe(2)–O(5)	78.5(1)
Fe(2)–C(4)	1.763(9)	Fe(2)–Fe(1)–C(1)	99.5(2)
P(1)–C(5)	1.862(8)	Fe(2)–Fe(1)–C(2)	152.3(3)
P(2)–C(5)	1.846(5)	Fe(1)–Fe(2)–C(3)	102.2(2)
		Fe(1)–Fe(2)–C(4)	153.0(2)
		Fe(1)–P(3)–Fe(2)	70.2(1)
		Fe(1)–O(5)–Fe(2)	68.7(1)
		P(1)–C(5)–P(2)	114.7(4)

high-temperature thermolysis. Upon attempted chromatography of **1** on alumina a gradual colour change from yellow to orange occurs upon elution with a dichloromethane–light petroleum mixture. Elution from the column affords the bridging-hydroxide complex $[Fe_2(CO)_4(\mu\text{-}OH)(\mu\text{-}PPh_2)(\mu\text{-}dppm)]$ **3** in 86% yield. Characterisation as a hydroxide complex is made on the basis of the ^1H NMR spectrum, the hydroxyl proton appearing as a well resolved signal at δ −2.75 (dt, *J* 6.0, 8.4 Hz). The chemical shift compares well with that of δ −2.86 found for the related diiron species $[Fe_2(CO)_6(\mu\text{-}OH)\{\mu\text{-}P(C_6H_4Me\text{-}p)_2\}]$.[6] In the ^{31}P NMR spectrum the *trans* orientation of phosphido and diphosphine moieties is clearly shown by their large coupling constant of 112 Hz. The mode of formation of **3**, a result of the replacement of carbon monoxide and hydride moieties by the three-electron hydroxide ligand, was investigated in a series of experiments. Addition of alumina to a toluene solution of **1** does not give **3** even after 2 weeks, nor does addition of deoxygenated water. Exposure of solutions to air results only in rapid decomposition. Addition of trimethylamine *N*-oxide hydrate, $Me_3NO\cdot 2H_2O$, to a toluene solution of **1** did, however, result in the slow formation of **3** over 2 weeks. Thus initial carbon monoxide loss may be a prerequisite for this process, the decarbonylated intermediate later reacting with water. In related work the unstable hydride complex $[Fe_2(CO)_7(\mu\text{-}H)(\mu\text{-}PPh_2)]$ was converted into the hydroxide upon addition of dioxygen.[7] Indeed, purging a solution of **1** with dioxygen led to the formation of **3**, albeit in low yield. While the mode of formation of **3** upon chromatography is not well understood, it possibly involves the initial adsorption of **1** onto the alumina support. Thus for example, adsorption of osmium dodecacarbonyl onto silica leads to the silica-anchored hydrido cluster $[Os_3(CO)_{10}(\mu\text{-}H)(\mu\text{-}OSi\text{–})]$, which while stable up to 423 K, can be chemically displaced by hydrogen fluoride to give high yields of $[Os_3(CO)_{10}(\mu\text{-}H)(\mu\text{-}OH)]$.[8]

Thermolysis of complex **1** with diphenylphosphine results in a rapid colour change from yellow to orange with the isolation after chromatography of $[Fe_2(CO)_4(\mu\text{-}PPh_2)_2(\mu\text{-}dppm)]$ **4** in 53% yield. At −20 °C the ^{31}P NMR spectrum (in CD_2Cl_2) shows sharp resonances at δ 170.1 (dt, *J* 115, 45) and 129.6 (*J* 115, 45 Hz), assigned to the inequivalent phosphido-bridges, while the diphosphine appears at δ 49.9 (t, *J* 45 Hz). In the proton spectrum at low temperature the two methylene protons of the diphosphine are inequivalent. Thermolysis of **1** in the presence of dicyclohexylphosphine similarly results in hydrogen loss and the formation of $[Fe_2(CO)_4(\mu\text{-}PPh_2)\{\mu\text{-}P(C_6H_{11})_2\}(\mu\text{-}dppm)]$ **5** in 49% yield. This latter reaction is somewhat slower than that with diphenylphosphine. The reduced reactivity of dicyclohexyl- *versus* diphenyl-phosphine has previously been noted and is a result of the increased steric demands of the former.[9] At room temperature the ^{31}P NMR spectrum of **5** shows two well resolved phosphido-bridge resonances at δ 209.7 (dt, *J* 102, 47) and 146.6 (dt, *J* 102, 43 Hz), and a third resonance attributed to the diphosphine at δ 69.9 (t, *J* 46 Hz). On the basis of these data it is not possible to deduce the relative positions of the phosphorus-containing ligands, but on steric grounds it is anticipated that the relatively bulky cyclohexyl substituents will occupy the less sterically crowded site *trans* to the diphosphine ligand. While in the absence of structural data we have been unable to confirm this, the regioselectivity of the reaction (only one isomer is produced) is supportive of this supposition. A number of earlier reports document the synthesis of complexes closely related to **4** and **5**. Thus $[Fe_2(CO)_4(PR_3)_2(\mu\text{-}PMe_2)_2]$ (R = Ph or Et) are synthesised upon photochemical substitution of the parent hexacarbonyl,[10] while $[Fe_2(CO)_4(PBu^n_3)_2(\mu\text{-}PPh_2)_2]$ is produced *via* an analogous thermal substitution.[11] It is noteworthy that these derivatives are believed to involve substitution of carbonyls *trans* to the metal–metal bond, an option clearly not available to the dppm ligand. A further point of note is the observation of the large phosphorus–phosphorus coupling constants between the phosphido-bridge moieties (**2**, 153; **4**, 115; **5**, 102 Hz). Previous workers have explored this phenomenon indirectly using proton NMR data.[12,13] Thus for example the phosphorus–phosphorus coupling constant of $[Fe_2(CO)_6(\mu\text{-}PMe_2)_2]$ has been estimated at 85 ± 10 Hz.[12] The inequivalence of the phosphido-bridge moieties here allows for the first direct measurement in a complex of the type $[Fe_2(CO)_6(\mu\text{-}PR_2)_2]$, although large phosphorus–phosphorus coupling constants have recently been reported for the complexes $[Fe_2(CO)_6(\mu\text{-}PR_2)(\mu\text{-}PR')]$ (R = Ph, R′ = C_6H_{11} or Bu^t; R = Me, R′ = Bu^t).[14] We considered that the magnitude of this coupling constant may be inversely related to the interatomic distance between the phosphorus atoms, however this is not borne out from the solid-state structures of **2** [P(2) ··· P(3) 2.925 Å] and **4** [P(1) ··· P(2) 2.871 Å].

Solid-state Structures.—The solid-state structures of complexes **2**–**4** have been elucidated by X-ray crystallography, the result being summarised in Tables 1–3 and Figs. 1–3 respectively. The structure of $[Fe_2(CO)_5(\mu\text{-}PPh_2)(\mu\text{-}PhPCH_2PPh_2)]$ **2** confirms the thermolytic loss of benzene. The diiron vector [Fe(1)–Fe(2) 2.699(2) Å] is bridged somewhat asymmetrically by a diphenylphosphido group [Fe(1)–P(3) 2.195(3), Fe(2)–P(3) 2.287(3) Å], and symmetrically by a second phosphido moiety [Fe(1)–P(2) 2.226(3), Fe(2)–P(2) 2.227(3) Å] formed *via* cleavage of a phenyl group from the original dppm ligand. Thus this phosphido-bridge carries both a phenyl substituent and the more unusual CH_2PPh_2 group, the phosphorus of which is co-ordinated to one of the iron centres [Fe(1)–P(1) 2.224(3) Å], lying *trans* to the diphenylphosphido moiety [P(1)–Fe(1)–P(3) 149.9(3)°]. The angles subtended by the phosphido ligands and the diiron vector are surprisingly similar [Fe(1)–P(2)–Fe(2) 74.6(1), Fe(1)–P(3)–Fe(2) 74.0(1)°] and correspond well with those found in related phosphido-

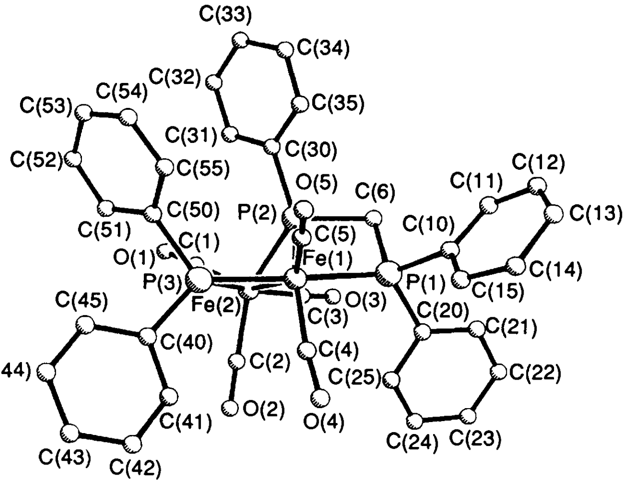

Fig. 1 Crystal structure of $[Fe_2(CO)_5(\mu\text{-}PPh_2)(\mu\text{-}PhPCH_2PPh_2)]$ **2**

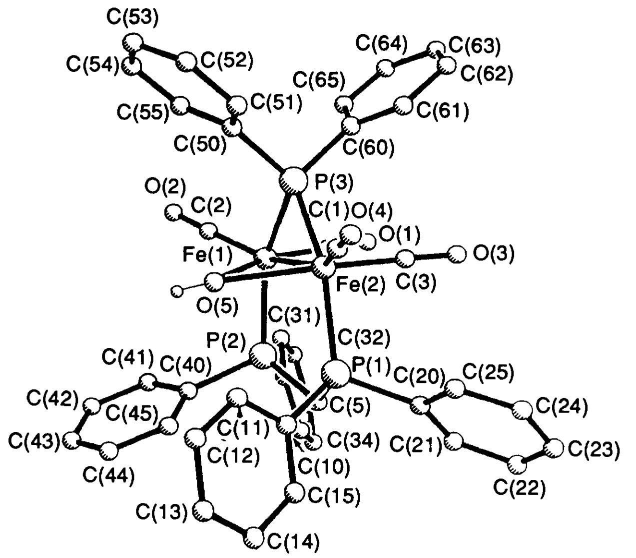

Fig. 2 Crystal structure of $[Fe_2(CO)_4(\mu\text{-}OH)(\mu\text{-}PPh_2)(\mu\text{-}dppm)]$ **3**

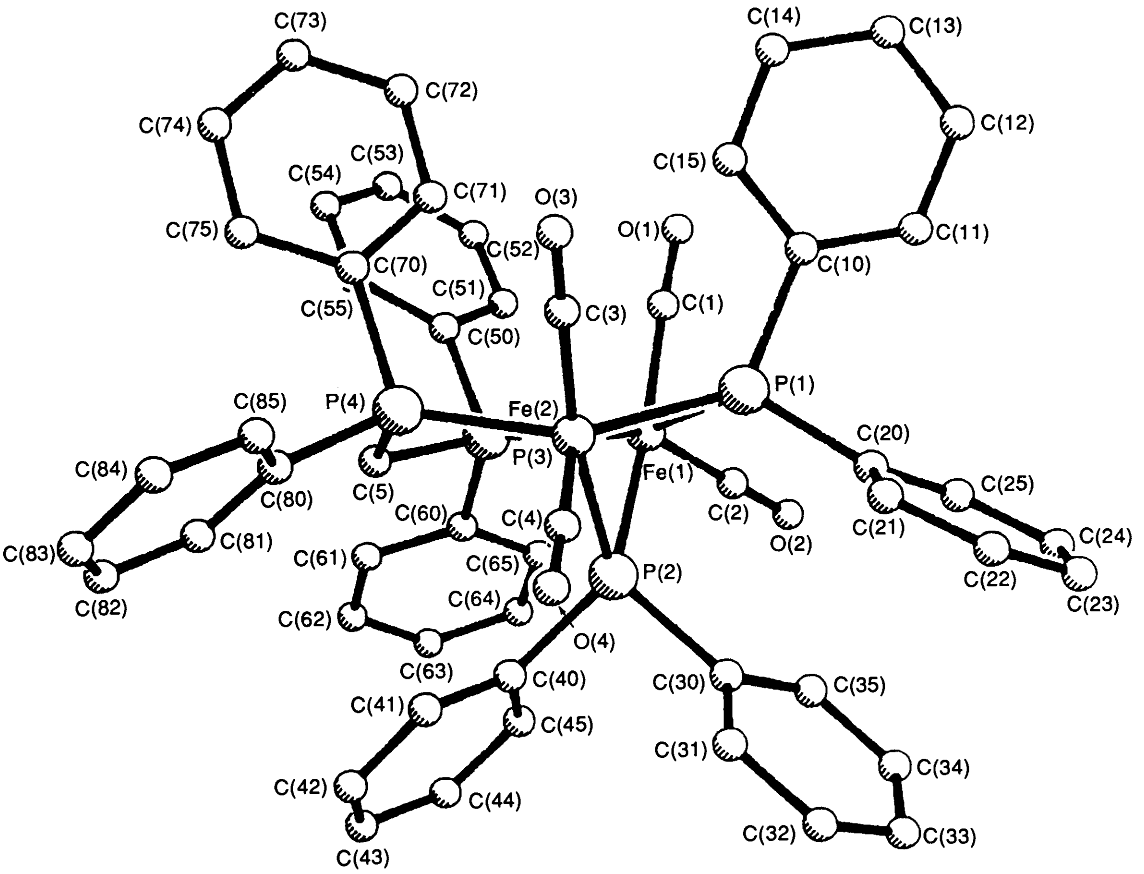

Fig. 3 Crystal structure of $[Fe_2(CO)_4(\mu\text{-}PPh_2)_2(\mu\text{-}dppm)]$ **4**

bridged diiron complexes. Substitution of a phenyl group for the metal-bound CH_2PPh_2 moiety thus leads only to a slight distortion of the geometry about phosphorus, the angles subtended by the carbon substituents at P(3) [C(40)–P(3)–C(50) 103.1°] and P(2) [C(6)–P(2)–C(30) 105.4°] being similar. One consequence of the metal binding of P(1) is the reduced P(1)–C(6)–P(2) angle of 91.9(5)° which allows for the close contact of the two phosphorus atoms, P(1) $\cdots$ P(2) 2.661(4) Å. The orientation of the μ-$PhPCH_2PPh_2$ ligand is similar to that found at the ruthenium–rhodium centre in [(dppm)PhRu(μ-H)(μ-Ph_2PCH_2PPh)Rh(cod)] which also contains a small P–C–P angle of 85.25°.[2] The ligand has also been characterised at triruthenium centres,[3,4] however here the phosphido moiety bridges two metal atoms while the phosphine substituent co-ordinates to the third. This mode of co-ordination allows for a considerable opening up of the P–C–P angle, measured at 106.70(11)° in [$Ru_3(CO)_9$(μ-H)($μ_3$-$PhPCH_2PPh_2$)].[3]

The hydroxide complex [$Fe_2(CO)_4$(μ-OH)(μ-PPh_2)(μ-dppm)] **3** was structurally characterised as its dichloromethane solvate. The diiron vector [Fe(1)–Fe(2) 2.546(1) Å] is bridged symmetrically by a dppm ligand [Fe(1)–P(2) 2.250(2), Fe(2)–P(1) 2.240(2) Å], but somewhat asymmetrically by a diphenylphosphido moiety [Fe(1)–P(3) 2.223(2), Fe(2)–P(3) 2.202(2) Å] and the hydroxide group [Fe(1)–O(5) 2.224(4), Fe(2)–O(5) 2.288(3) Å]. The two phosphorus-containing ligands are found *trans* to one another, presumably as a result of steric requirements, while the hydroxide lies *cis* to both. The angle subtended by the phosphido-bridge and the diiron vector [Fe(1)–P(3)–Fe(2) 70.2(1)°] is within the expected range. More surprising is the angle subtended by the hydroxide ligand [Fe(1)–O(5)–Fe(2) 68.7(1)°] when compared to that of 79.1(2)° found in the related diiron complex [$Fe_2(CO)_6$(μ-OH){μ-P(C_6H_4Me-*p*)$_2$}].[6] While at first sight this appears significant, it is simply a result of the decreased iron–oxygen bond lengths in the hexacarbonyl [Fe–O(average) 1.972 Å] as compared to those in **3** [Fe–O(average) 2.256 Å]. This effect is probably a consequence of the increased electron density at the diiron centre as a result of dicarbonyl substitution for dppm, thus decreasing the donor ability of the hydroxide.

The bis(phosphido)-bridged complex [$Fe_2(CO)_4$(μ-PPh_2)$_2$-(μ-dppm)] **4** consists of two iron atoms 2.713(2) Å apart bridged by inequivalent diphenylphosphido moieties and a dppm ligand. Both the phosphido groups show a small degree of asymmetry upon bridging the metal–metal vector [Fe(1)–P(2) 2.242(2), Fe(2)–P(2) 2.250(2); Fe(1)–P(1) 2.232(2), Fe(2)–P(1) 2.218(2) Å]. The diphosphine ligand, however, bridges quite asymmetrically [Fe(1)–P(3) 2.271(2), Fe(2)–P(4) 2.223(2) Å]. Of the phosphido-bridges, one lies *trans* to the diphosphine [P(1)–Fe(1)–P(3) 146.2(1), P(1)–Fe(2)–P(4) 136.2(1)°], and the angle between them and the diiron vector of 107.8° is opened up somewhat with respect to the angle of 100.0° found in [$Fe_2(CO)_6$(μ-PPh_2)$_2$].[15] In view of the solid-state structure it is noteworthy that despite the quite different angles that the phosphido-bridges subtend with the diphosphine, both phosphorus–phosphorus coupling constants are similar (indistinguishable within experimental error). Carty[16] has previously shown that the ^{31}P NMR resonance frequency of phosphido-bridge ligands in complexes [$Fe_2(CO)_6$(μ-PPh_2)(μ-X)] (X = three-electron donor ligand) correlates well with the Fe–P–Fe angle subtended by the ligand, such that this increases as downfield movement in chemical shift occurs.[16] In this context it is interesting that the difference in chemical shift is greater than 40 ppm for the two phosphido-bridge ligands in **4** when the Fe–P–Fe angles vary by only 0.8° [Fe(1)–P(1)–Fe(2) 75.1(1), Fe(1)–P(2)–Fe(2) 74.3(1)°]. These are opened up with respect to those found in the parent complex [$Fe_2(CO)_6$(μ-PPh_2)$_2$] (average 72.0°),[15] probably as a consequence of the longer iron–iron distance in **4** [2.713(2) Å] as compared to that in the former [2.623(2) Å]. On the basis of Carty's earlier work an approximate difference in chemical shift of 16 ppm is predicted for a 0.8° change in angle. Clearly other effects are important in chemical shift prediction. While on the basis of the phosphorus–phosphorus coupling constants it is not possible definitely to assign resonances in the phosphido-bridge region of the ^{31}P NMR spectrum, it is nevertheless tempting to attribute the low-field resonance to P(1).

Fluxional Behaviour in Solution.—No temperature dependency is observed in the NMR spectral properties of complexes **2** and **3** between −100 and +100 °C. In contrast the spectra of the bis(phosphido)-bridged complexes **4** and **5** undergo considerable changes within this range, which may be attributed to two different fluxional processes. Thus for **4**, raising the temperature to 100 °C results in coalescence of the signals of inequivalent phosphido groups, conveniently monitored by ^{31}P NMR spectroscopy, the main feature being the collapse of signals at δ 170.1 and 129.6 into a single broad resonance. The same process can be followed by ^1H NMR spectroscopy. Here coalescence of the resonances of the initially inequivalent methylene protons occurs at 40 °C. From these data free energies of activation of 62 ± 1 and 60 ± 1 kJ mol^{-1} respectively can be estimated indicating that both spectral observations are consistent with the same fluxional process. We attribute these observations to a 'rocking' of the two phosphido moieties as shown in Scheme 2. Thus in the transition state the molecule possesses a plane of symmetry (which includes the diiron vector and the diphosphine backbone) thus equivalencing the phosphido-bridges. It is noteworthy however that the data also fit a process in which the phosphido-bridges are interconverted *via* a bridge–terminal–bridge mechanism. A similar mechanistic ambiguity surrounds the fluxionality of the unsubstituted hexacarbonyl complexes [$Fe_2(CO)_6$(μ-PR_2)$_2$]. Here a 'butterfly' mechanism appears to have gained credence[17] in which the Fe_2P_2 core is planar in the transition state. However attempts to distinguish between this and a bridge-opening mechanism have been the subject of a number of studies,[18,19] and to our knowledge the definitive experiment has yet to be performed. A 'butterfly' mechanism is easily ruled out in **4** since this involves a movement of the diphosphine moiety from one side of the molecule to the other.

The ^{31}P and ^1H NMR spectra of complex **5** remain essentially unchanged between room temperature and 100 °C. In the former, however, reduction of the temperature to −110 °C results in the splitting of the diphosphine resonance at δ 69.9 into two new signals at 68.0 (ddd, *J* 114, 52, 30) and 61.3 (ddd, *J* 114, 57, 40 Hz). The phosphido-bridge resonances vary only slightly with temperature, the coupling constant between them remaining virtually unchanged. It is however significant that the high-field signal develops a further doublet coupling, δ 151.0 (ddd, *J* 102, 57, 30 Hz). Such changes are not consistent with phosphido-bridge fluxionality, but rather are attributed to a process in which the mirror plane bisecting the iron–iron bond and incorporating the phosphorus atoms of the phosphido-bridges and the methylene carbon of the diphosphine ligand is lost. Careful inspection of the X-ray crystal structure of **4** shows that at room temperature this is indeed the situation observed. Thus we attribute these observations to a process in which the phosphorus atoms of the dppm ligand 'twist' backwards and forwards (Scheme 3). This is consistent with observed changes in the ^1H NMR spectrum, since at −85 °C while the cyclohexyl resonances are virtually unchanged the phenyl region is considerably broadened. From the coalescence temperature of −78 °C the free energy of activation can be estimated at 34 ± 1 kJ mol^{-1}.

Experimental

General Comments.—All reactions were carried out under a nitrogen atmosphere using predried solvents unless otherwise stated. The NMR spectra were recorded on a Varian VXR 400 spectrometer, IR spectra as KBr disks on a Perkin Elmer 983 spectrometer. Chromatography was carried out on columns

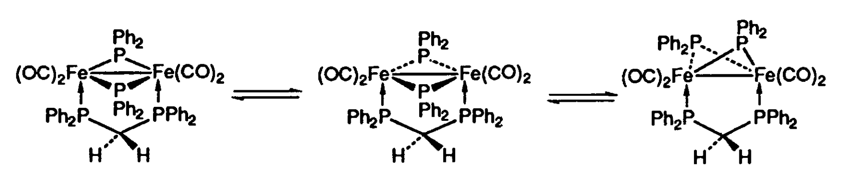

Scheme 2 Interconversion of phosphido-bridges and methylene protons in complex 4 *via* 'rocking' motion

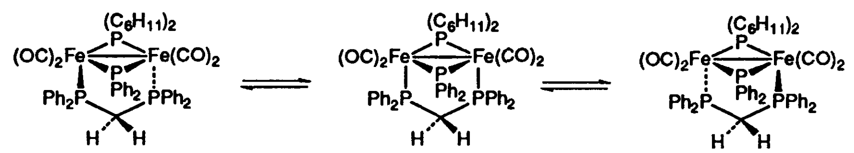

Scheme 3 Interconversion of the ends of the diphosphine in complex 5 *via* 'twisting' motion

Table 4 Crystallographic data for complexes **2**–**4**

	2	**3**	**4**
Formula	$C_{36}H_{27}Fe_2O_5P_3$	$C_{42}H_{35}Cl_2Fe_2O_5P_3$	$C_{53}H_{42}Fe_2O_4P_4$
M	744.2	895.3	978.6
Crystal symmetry	Monoclinic	Triclinic	Monoclinic
Space group	$P2_1/c$	$P\bar{1}$	$P2_1/n$
a/Å	14.8348(53)	11.9981(30)	13.6589(53)
b/Å	9.7766(28)	12.3020(25)	18.1858(50)
c/Å	23.3866(83)	16.8524(38)	18.3919(47)
α/°	90.0	72.380(17)	90.0
β/°	90.349(29)	75.990(18)	91.400(27)
γ/°	90.0	63.780(16)	90.0
U/Å^3	3391.79	2109.64	4576.18
Z	4	2	4
F(000)	1520	916	2016
D_c/g cm^{-3}	1.46	1.41	1.42
Crystal size/mm	0.50 × 0.40 × 0.18	0.68 × 0.40 × 0.18	0.62 × 0.30 × 0.10
μ(Mo-Kα)/cm^{-1}	1.03	0.97	8.16
Orientation reflections (no. range)	28, $11 \leqslant 2\theta \leqslant 24$	28, $16 \leqslant 2\theta \leqslant 25$	30, $10 \leqslant 2\theta \leqslant 26$
Data measured	6833	8270	9041
Unique data	5877	7817	8565
No. unique with $I \geqslant 3.0\sigma(I)$	2271	5206	4517
No. of parameters	265	487	568
R^a	0.081	0.063	0.050
R'^b	0.086	0.070	0.052
Weighting scheme	$w^{-1} = \sigma^2(F) + 0.009\,458F^2$	$w^{-1} = \sigma^2(F) + 0.001\,420F^2$	$w^{-1} = \sigma^2(F) + 0.001\,033F^2$
Largest shift/e.s.d. in the final cycle	0.008	0.16	0.09
Largest peak/e Å^{-3}	0.69	1.14	0.48

^{a} $R = \Sigma(|F_o| - |F_c|)/\Sigma|F_o|$. ^{b} $R' = \Sigma w^{\frac{1}{2}}(|F_o| - |F_c|)/\Sigma w^{\frac{1}{2}}|F_o|$.

of deactivated alumina (6% w/w water). Elemental analysis was performed within the chemistry department of University College. The compound $[Fe_2(CO)_4(\mu\text{-}H)(\mu\text{-}CO)(\mu\text{-}PPh_2)(\mu\text{-}dppm)]$ **1** was prepared as previously reported.[1] Diphenylphosphine and dicyclohexylphosphine were purchased from Aldrich and used as supplied.

Syntheses.—$[Fe_2(CO)_5(\mu\text{-}PPh_2)(\mu\text{-}PhPCH_2PPh_2)]$ **2**.—A toluene solution (100 cm^3) of complex **1** (1.00 g, 1.30 mmol) was refluxed for 2 h and a colour change from golden brown to orange was noted. Removal of the solvent under reduced pressure gave an orange solid which was chromatographed on alumina. Elution with light petroleum (b.p. 40–60 °C)–dichloromethane (9:1) gave a yellow band which afforded $[Fe_2(CO)_5(\mu\text{-}PPh_2)(\mu\text{-}PhPCH_2PPh_2)]$ (0.85 g, 75%). Crystals suitable for X-ray diffraction were grown upon slow diffusion of methanol into a dichloromethane solution (Found: C, 57.10; H, 3.65; P, 12.50. Calc. for $C_{36}H_{27}Fe_2O_5P_3$: C, 58.05; H, 3.65; P, 12.50%). NMR ($CDCl_3$): ^1H, δ 7.8–6.6 (m, 25 H, Ph) and 4.37 (dt, *J* 11.2, 3.0, PCH_2P); ^{31}P, δ 171.1 (dd, *J* 153, 50, μ-PPh_2), 103.7 (dd, *J* 153, 104, μ-PPh) and 37.4 (dd, *J*, 104, 50, PPh_2)^{13}C, δ 219.4 (q, *J* 7, CO), 217.8 (d, *J* 18, CO), 215.6 (t, *J* 4, 3CO), 140–126 (m, Ph) and 30.1 (t, *J* 30 Hz, PCH_2P). IR (CH_2Cl_2): 2022m, 1972s, 1948m and 1916m cm^{-1}.

$[Fe_2(CO)_4(\mu\text{-}OH)(\mu\text{-}PPh_2)(\mu\text{-}dppm)]$ **3**. Complex **1** (1.00 g, 1.30 mmol) was adsorbed onto alumina and chromatographed. Elution with light petroleum–dichloromethane (9:1) produced a yellow band which changed to orange as it moved down the column. The solvent was subsequently removed to yield complex **3** as an orange solid (0.95 g, 86%). Crystals suitable for X-ray diffraction were grown from slow diffusion of methanol into a dichloromethane solution (Found: C, 55.20; H, 3.80; P, 10.15. Calc. for $C_{41}H_{33}Fe_2O_5P_3$: C, 56.35; H, 3.95; P, 10.40%). NMR ($CDCl_3$): ^1H, δ 7.8–7.2 (30 H, m, Ph), 3.19 (1 H, q, *J* 7.2, C*H*H), 2.82 (1 H, q, *J* 7.2, CH*H*) and −2.75 (1 H, dt, *J* 6.0, 8.4, μ-OH); ^{31}P, δ 149.4 (t, *J* 112, μ-PPh_2) and 50.9 (d, *J* 112 Hz, PCH_2P). IR (CH_2Cl_2): 1978m, 1950s and 1910m cm^{-1}.

$[Fe_2(CO)_4(\mu\text{-}PPh_2)_2(\mu\text{-}dppm)]$ **4**. A toluene solution (100 cm^3) of complex **1** (1.00 g, 1.30 mmol) and diphenylphosphine (0.3 g, 1.61 mmol) was refluxed for 2 h resulting in a change from golden brown to orange. After removal of the solvent under reduced pressure the orange solid produced was chromatographed on alumina. Elution with light petroleum–dichloromethane (9:1) afforded complex **3** (0.45 g, 42%). Further elution with light petroleum–dichloromethane (4:1) gave an orange band which afforded **4** (0.75 g, 53%) as a bright orange solid. Crystals suitable for X-ray diffraction were grown upon slow diffusion of methanol into a dichloromethane solution (Found:

Table 5 Atomic coordinates (× 10^4) for complex **2**

Atom	*x*	*y*	*z*	Atom	*x*	*y*	*z*
Fe(1)	7921(1)	1780(1)	1886(1)	C(21)	6031(8)	670(12)	3497(5)
Fe(2)	6468(1)	2997(1)	1408(1)	C(22)	5507(9)	1343(14)	3909(6)
P(1)	7154(2)	588(3)	2530(1)	C(23)	5472(10)	2720(14)	3922(6)
P(2)	6792(2)	773(1)	1417(1)	C(24)	5905(9)	3489(14)	3517(5)
P(3)	7941(2)	3100(3)	1127(1)	C(25)	6420(9)	2839(11)	3103(5)
O(1)	5581(7)	3642(11)	319(4)	C(30)	6768(7)	−397(10)	805(4)
O(2)	6480(7)	5726(9)	1937(5)	C(31)	6348(8)	−33(12)	306(5)
O(3)	4814(7)	2287(11)	2019(5)	C(32)	6293(9)	−915(12)	−152(5)
O(4)	8748(7)	3494(9)	2771(4)	C(33)	6654(10)	−2207(14)	−106(6)
O(5)	9507(6)	77(9)	1756(4)	C(34)	7078(10)	−2604(17)	406(6)
C(1)	5932(9)	3376(11)	734(5)	C(35)	7131(9)	−1681(13)	848(6)
C(2)	6500(7)	4654(12)	1724(5)	C(40)	8563(7)	4698(10)	1108(4)
C(3)	5484(8)	2583(13)	1803(5)	C(41)	8614(7)	5522(11)	1601(5)
C(4)	8424(9)	2877(11)	2398(5)	C(42)	9121(9)	6694(12)	1630(5)
C(5)	8859(8)	720(11)	1812(5)	C(43)	9590(10)	7103(14)	1156(6)
C(6)	6365(7)	−250(10)	2028(4)	C(44)	9566(9)	6316(13)	661(5)
C(10)	7749(7)	−758(11)	2911(4)	C(45)	9066(9)	5130(13)	633(5)
C(11)	7441(9)	−2107(12)	2944(5)	C(50)	8160(7)	2350(10)	418(4)
C(12)	7925(10)	−3071(14)	3227(6)	C(51)	7764(8)	2985(11)	−71(5)
C(13)	8707(13)	−2752(19)	3515(7)	C(52)	7893(9)	2400(14)	−605(5)
C(14)	9019(16)	−1358(22)	3521(9)	C(53)	8394(9)	1204(15)	−665(6)
C(15)	8519(11)	−403(18)	3186(6)	C(54)	8758(8)	643(13)	−198(5)
C(20)	6503(7)	1401(11)	3088(4)	C(55)	8653(8)	1168(12)	347(5)

Table 6 Atomic coordinates (× 10^4) for complex **3**

Atom	*x*	*y*	*z*	Atom	*x*	*y*	*z*
Fe(1)	2 448(1)	7 218(1)	7 865(1)	C(30)	1 794(5)	4 776(5)	7 671(3)
Fe(2)	4 629(1)	7 130(1)	7 221(1)	C(31)	547(6)	5 604(6)	7 621(4)
P(1)	5 536(1)	5 110(1)	7 194(1)	C(32)	−273(6)	5 265(8)	7 393(5)
P(2)	2 874(1)	5 200(1)	8 005(1)	C(33)	140(7)	4 113(8)	7 216(5)
P(3)	3 000(2)	8 827(1)	7 453(1)	C(34)	1 343(7)	3 312(7)	7 265(4)
O(1)	1 316(6)	7 977(5)	6 335(3)	C(35)	2 179(6)	3 623(6)	7 496(4)
O(2)	175(5)	8 003(7)	9 036(4)	C(40)	3 012(6)	4 239(5)	9 071(3)
O(3)	4 451(5)	7 806(5)	5 437(3)	C(41)	1 927(7)	4 260(7)	9 615(4)
O(4)	6 796(5)	7 711(5)	7 038(3)	C(42)	2 012(9)	3 559(8)	10 428(5)
O(5)	4 008(3)	6 533(3)	8 620(2)	C(43)	3 130(10)	2 837(8)	10 713(5)
C(1)	1 762(7)	7 673(5)	6 940(4)	C(44)	4 184(9)	2 807(8)	10 293(5)
C(2)	1 073(7)	7 673(7)	8 585(4)	C(45)	4 157(8)	3 497(7)	9 382(5)
C(3)	4 518(6)	7 549(6)	6 138(4)	C(50)	3 036(7)	9 611(6)	8 218(4)
C(4)	5 944(6)	7 462(6)	7 140(4)	C(51)	4 034(9)	9 886(7)	8 169(6)
C(5)	4 356(5)	4 434(5)	7 369(4)	C(52)	4 047(11)	10 494(8)	8 751(7)
C(10)	6 671(5)	4 018(6)	7 931(4)	C(53)	3 075(15)	10 805(9)	9 370(7)
C(11)	6 922(7)	4 443(7)	8 525(4)	C(54)	2 101(16)	10 533(12)	9 414(7)
C(12)	7 755(9)	3 612(8)	9 078(6)	C(55)	2 062(11)	9 941(9)	8 840(6)
C(13)	8 325(10)	2 378(9)	9 063(6)	C(60)	2 333(6)	10 141(5)	6 599(4)
C(14)	8 093(9)	1 956(8)	8 481(6)	C(61)	3 090(7)	10 587(6)	5 955(5)
C(15)	7 274(7)	2 785(6)	7 914(5)	C(62)	2 561(10)	11 602(8)	5 300(5)
C(20)	6 454(5)	4 743(5)	6 200(3)	C(63)	1 304(10)	12 102(8)	5 280(6)
C(21)	6 269(6)	4 089(7)	5 742(4)	C(64)	536(9)	11 669(7)	5 910(7)
C(22)	7 044(7)	3 841(8)	5 001(5)	C(65)	1 043(7)	10 703(6)	6 568(5)
C(23)	7 949(7)	4 310(7)	4 683(4)	C(70)	1 812(16)	10 251(14)	3 504(9)
C(24)	8 116(7)	4 980(7)	5 122(4)	Cl(1)	1 754(4)	10 578(5)	2 517(4)
C(25)	7 399(6)	5 204(6)	5 863(4)	Cl(2)	3 587(11)	9 122(6)	3 581(6)

C, 64.55; H, 4.10; P, 12.70. Calc. for $C_{53}H_{42}Fe_2O_4P_4$: C, 65.05; H, 4.30; P, 12.70%). ^{1}H NMR ($CDCl_3$, 253 K): δ 8.0–6.3 (m, 40 H, Ph), 3.52 (br, 1 H, C*H*H) and 2.53 (dt, *J* 14.0, 10.1 Hz, 1 H, CH*H*); ^{31}P (CD_2Cl_2, 253 K), δ 170.1 (dt, *J* 115, 45, μ-PPh_2), 129.6 (dt, *J* 115, 45, μ-PPh_2), 49.9 (t, *J* 45, PCH_2P). IR (CH_2Cl_2): 1974m, 1947s and 1907m cm^{-1}.

[$Fe_2(CO)_4(\mu\text{-}PPh_2)\{\mu\text{-}P(C_6H_{11})_2\}(\mu\text{-dppm})$] **5**. A toluene solution (100 cm^3) of complex **1** (1.00 g, 1.30 mmol) and dicyclohexylphosphine (0.3 g, 1.51 mmol) was refluxed for 5 h resulting in a change from golden brown to orange. After removal of the solvent under reduced pressure the orange solid produced was chromatographed on alumina. Elution with light petroleum–dichloromethane (4:1) gave a yellow band which afforded [$Fe_2(CO)_4(\mu\text{-}PPh_2)\{\mu\text{-}P(C_6H_{11})_2\}(\mu\text{-dppm})$] **5** (0.7 g, 49%) as a yellow solid (Found: C, 61.60; H, 5.05; P, 12.30. Calc. for $C_{53}H_{54}Fe_2O_4P_4{\cdot}0.5CH_2Cl_2$: C, 62.15; H, 5.30; P, 12.00%). NMR: ^{1}H ($C_6D_5CD_3$), δ 8.2–6.1 (m, 30 H, Ph), 2.41 (dt, 1 H, *J* 11.8, 4.4, PC*H*HP), 2.33 (t, 1 H, *J* 11.8, PCH*H*P) and 3.3–1.1 (m, 22 H, C_6H_{11}); ^{31}P (CD_2Cl_2–CF_2HCl, 163 K), δ 213.4 [dt, *J* 102, 47, μ-$P(C_6H_{11})_2$], 151.0 (ddd, *J* 102, 57, 30, μ-PPh_2), 68.0 (ddd, *J* 114, 52, 30, 0.5dppm) and 61.3 (ddd, *J* 114, 57, 40 Hz, 0.5dppm). IR (CH_2Cl_2): 1962m, 1937s and 1899m cm^{-1}.

Reactions of Complex **1** *with Molecular Oxygen and* $Me_3NO{\cdot}2H_2O$.—Oxygen gas was bubbled through a toluene solution (50 cm^3) of complex **1** (100 mg, 0.13 mmol) for 1 h after which time the IR spectrum indicated the formation of small amounts of **3** (*ca.* 10%). Extensive decomposition was also noted.

Addition of $Me_3NO{\cdot}2H_2O$ (70 mg, 0.63 mmol) to a toluene solution (10 cm^3) of complex **1** (100 mg, 0.13 mmol) resulted in

Table 7 Atomic coordinates (× 10^4) for complex **4**

Atom	*x*	*y*	*z*
Fe(1)	519(1)	8 574(1)	1 162(1)
Fe(2)	−627(1)	7 715(1)	1 993(2)
P(1)	−891(1)	8 874(1)	1 670(1)
P(2)	829(1)	8 210(1)	2 309(1)
P(3)	1 436(1)	7 658(1)	689(1)
P(4)	−42(1)	6 711(1)	1 467(1)
O(1)	−336(4)	8 895(3)	−271(3)
O(2)	1 702(4)	9 901(3)	1 123(3)
O(3)	−2 620(3)	7 287(3)	1 611(3)
O(4)	−967(4)	7 280(4)	3 488(3)
C(1)	−27(5)	8 748(3)	293(4)
C(2)	1 247(5)	9 372(3)	1 138(3)
C(3)	−1 825(5)	7 461(3)	1 726(3)
C(4)	−829(5)	7 463(4)	2 894(4)
C(5)	1 204(4)	6 775(3)	1 130(3)
C(10)	−1 917(4)	9 169(3)	1 057(3)
C(11)	−2 265(5)	9 877(4)	1 050(4)
C(12)	−3 025(6)	10 083(5)	585(5)
C(13)	−3 445(6)	9 607(5)	112(5)
C(14)	−3 097(5)	8 894(5)	100(4)
C(15)	−2 341(5)	8 677(4)	570(4)
C(20)	−1 037(4)	9 560(3)	2 395(3)
C(21)	−1 589(5)	9 373(4)	2 987(4)
C(22)	−1 791(7)	9 886(5)	3 521(5)
C(23)	−1 418(7)	10 587(5)	3 470(5)
C(24)	−857(6)	10 770(4)	2 891(5)
C(25)	−664(5)	10 264(4)	2 360(4)
C(30)	933(4)	8 883(3)	3 059(3)
C(31)	670(6)	8 708(5)	3 750(4)
C(32)	763(6)	9 218(6)	4 318(4)
C(33)	1 129(6)	9 903(5)	4 194(5)
C(34)	1 406(6)	10 079(4)	3 512(5)
C(35)	1 319(5)	9 584(4)	2 950(4)
C(40)	1 867(4)	7 632(3)	2 612(3)
C(41)	1 738(5)	6 983(4)	2 984(3)
C(42)	2 540(7)	6 572(4)	3 215(4)
C(43)	3 464(7)	6 790(6)	3 086(5)
C(44)	3 609(5)	7 448(5)	2 716(4)
C(45)	2 810(4)	7 877(4)	2 486(3)
C(50)	1 312(4)	7 458(3)	−289(3)
C(51)	1 569(5)	8 010(4)	−772(3)
C(52)	1 572(5)	7 884(4)	−1 509(4)
C(53)	1 313(5)	7 208(5)	−1 785(4)
C(54)	1 060(6)	6 655(4)	−1 313(4)
C(55)	1 060(5)	6 778(4)	−573(3)
C(60)	2 785(4)	7 696(3)	726(3)
C(61)	3 348(5)	7 064(4)	730(4)
C(62)	4 350(5)	7 093(5)	748(5)
C(63)	4 809(5)	7 757(5)	719(4)
C(64)	4 276(5)	8 389(4)	676(4)
C(65)	3 260(5)	8 366(3)	687(3)
C(70)	−722(4)	6 402(3)	647(3)
C(71)	−1 083(5)	6 928(3)	172(3)
C(72)	−1 565(5)	6 732(4)	−469(4)
C(73)	−1 670(6)	6 006(4)	−647(4)
C(74)	−1 314(6)	5 482(4)	−175(4)
C(75)	−836(5)	5 666(3)	471(4)
C(80)	2(5)	5 858(3)	2 000(3)
C(81)	830(6)	5 443(4)	2 112(4)
C(82)	789(8)	4 806(5)	2 520(5)
C(83)	−64(8)	4 562(5)	2 799(5)
C(84)	−891(8)	4 960(5)	2 682(4)
C(85)	−859(5)	5 609(4)	2 296(4)

a slight colour change over 2 weeks. Infrared spectroscopy revealed the presence of **1** and **3**, with the latter being the major component (*ca.* 80%). Little decomposition was noted.

Crystal-structure Determinations.—An orange single crystal of $[Fe_2(CO)_5(\mu\text{-}PPh_2)(\mu\text{-}PhPCH_2PPh_2)]$ **2**, approximate size 0.50 × 0.40 × 0.18 mm, was mounted on a glass fibre. All geometric and intensity data were taken from this sample at 19 °C using an automated four-circle diffractometer (Nicolet R3mV) equipped with Mo-Kα radiation (λ = 0.710 73 Å). The lattice vectors were identified by application of the automatic indexing routine of the diffractometer to the positions of 28 reflections taken from a rotation photograph and centred by the diffractometer. The ω–2θ technique was used to measure 6833 reflections (5877 unique) in the range $5 \leqslant 2\theta \leqslant 50$. Three standard reflections (remeasured every 97 scans) showed no significant loss in intensity during data collection. The data were corrected for Lorentz and polarisation effects. The 2271 unique data with $I \geqslant 3.0\sigma(I)$ were used to solve and refine the structure in the monoclinic space group $P2_1/c$.

The structure was solved by direct methods and developed by using alternating cycles of least-squares refinement and Fourier-difference synthesis. The non-hydrogen atoms directly linked to the core of the molecule were refined anisotropically while the phenyl ring carbons were only isotropically refined. Hydrogens were placed in idealised positions (C–H 0.96 Å) and assigned a common isotropic thermal parameter (U = 0.08 Å^2). The final cycle of least-squares refinement included 265 parameters for 2271 variables and did not shift any parameter by more than 0.008 times its standard deviation. The final R values were 0.081 and 0.086, and the final Fourier difference map was featureless with no peaks greater than 0.69 e Å^{-3}. Structure solution used the SHELXTL PLUS program package[20] on a microVax II computer.

Crystallographic analyses of complexes **3** and **4** were carried out in an analogous manner, however all non-hydrogen atoms were refined anisotropically. All important crystallographic parameters are summarised in Table 4, atomic coordinates in Tables 5–7.

Additonal material available from the Cambridge Crystallographic Data Centre comprises H-atom coordinates, thermal parameters and remaining bond lengths and angles.

Acknowledgements

We thank University College for the award of a studentship (to M. H. L.).

References

1 G. Hogarth and M. H. Lavender, *J. Chem. Soc., Dalton Trans.*, 1992, 2759.

2 B. Delavaux, B. Chaudret, F. Dahan and R. Poilblanc, *Organometallics*, 1985, **4**, 935.

3 N. Lugan, J.-J. Bonnet and J. A. Ibers, *J. Am. Chem. Soc.*, 1985, **107**, 4484.

4 G. Lavigne, N. Lugan and J.-J. Bonnet, *Organometallics*, 1982, **1**, 1040.

5 N. M. Doherty, G. Hogarth, S. A. R. Knox, K. A. Macpherson, F. Melchior and A. G. Orpen, *J. Chem. Soc., Chem. Commun.*, 1986, 540; N. M. Doherty, G. Hogarth, S. A. R. Knox, K. A. Macpherson, F. Melchior, D. A. V. Morton and A. G. Orpen, *Inorg. Chim. Acta*, 1992, **198–200**, 257.

6 P. M. Treichel, W. K. Dean and J. C. Calabrese, *Inorg. Chem.*, 1973, **12**, 2908.

7 B. Walther, H. Hartung, H.-C. Böttcher, U. Baumeister, U. Böhland, J. Sieler, J. Reinhold, J. Ladriere and H.-M. Schiebel, *Polyhedron*, 1991, **10**, 2423.

8 C. Dossi, A. Fusi, M. Pizzotti and R. Psaro, *Organometallics*, 1990, **9**, 1994.

9 T. Blum, P. Braunstein, A. Tiripicchio and M. Tiripicchio Camellini, *Organometallics*, 1989, **8**, 2504; P. Braunstein, E. de Jesús, A. Dedieu, M. Lanfranchi and A. Tiripicchio, *Inorg. Chem.*, 1992, **31**, 399.

10 D. T. Thompson, *J. Organomet. Chem.*, 1965, **4**, 74.

11 J. N. Gerlach, S. L. McMullin and P. C. Ellgen, *Inorg. Chem.*, 1976, **15**, 1232.

12 R. E. Dessy, A. L. Rheingold and G. D. Howard, *J. Am. Chem. Soc.*, 1972, **94**, 746.

13 G. R. Davies, R. H. B. Mais, P. G. Owsten and D. T. Thompson, *J. Chem. Soc. A*, 1968, 1251; R. G. Hayter, *Inorg. Chem.*, 1964, **3**, 711.

14 B. Walther, H. Hartung, J. Reinhold, P. G. Jones, C. Mealli, H.-C. Böttcher, U. Baumeister, A. Krug and A. Möckel, *Organometallics*, 1992, **11**, 1542.

15 R. E. Ginsburg, R. K. Rothrock, R. G. Finke, J. P. Collman and L. F. Dahl, *J. Am. Chem. Soc.*, 1979, **101**, 6550.

16 A. J. Carty, *Adv. Chem. Ser.*, 1982, **192**, 163; A. J. Carty, C. A. Fyfe, M. Lettinga, S. Johnson and L. H. Randall, *Inorg. Chem.*, 1989, **28**, 4120.

17 D. F. Shriver and K. H. Whitmire, in *Comprehensive Organometallic Chemistry*, eds. G. Wilkinson and F. G. A. Stone, Pergamon, Oxford, 1982, vol. 4, p. 301.

18 R. D. Adams, F. A. Cotton, W. R. Cullen, D. L. Hunter and L. Mihichuk, *Inorg. Chem.*, 1975, **14**, 1395.

19 G. Grobe, *Z. Anorg. Allg. Chem.*, 1968, **321**, 32; R. D. Adams and F. A. Cotton, *J. Am. Chem. Soc.*, 1970, **92**, 5003.

20 G. M. Sheldrick, SHELXTL, University of Göttingen, 1985.

Received 13*th August* 1992; *Paper* 2/04402A